Materials Research Bulletin 119 (2019) 110568

Contents lists available at ScienceDirect

Materials Research Bulletin

journal homepage: www.elsevier.com/locate/matresbu

Investigating the effect of graphene on eutectic salt properties for thermal energy storage

Sumair Faisal Ahmed[a], Mohammad Khalid[b,*], Rashmi Walvekar[c,*], Mahesh Vaka[c], Nabisab Mujawar Mubarak[d], Ali Chamkha[e,f], Muhammad Khalid[a]

[a] Central Instrumentation Facility (CIF), Jamia Millia Islamia, New Delhi, 110025, India
[b] Graphene & Advanced 2D Materials Research Group (GAMRG), School of Science and Technology, Sunway University, 5, Jalan Universiti, Bandar Sunway, 47500 Subang Jaya, Selangor, Malaysia
[c] Sustainable Energy and Green Technology Research Group, Faculty of Innovation and Technology, School of Engineering, Taylor's University, 47500 Subang Jaya, Selangor, Malaysia
[d] Department of Chemical Engineering, Faculty of Engineering and Science, Curtin University, 98009, Sarawak, Malaysia
[e] Mechanical Engineering Department, Prince Sultan Endowment for Energy and Environment, Prince Mohammad Bin Fahd University, Al-Khobar 31952, Saudi Arabia
[f] RAK Research and Innovation Center, American University of Ras Al Khaimah, P.O. Box 10021, Ras Al Khaimah, United Arab Emirates

ARTICLE INFO

Keywords:
Thermal energy storage
Graphene
Heat capacity
Thermal conductivity
Eutectic salt

ABSTRACT

Enhancement of heat capacity and thermal conductivity with the dispersion of graphene nanoparticles into low-temperature eutectic salt was investigated. Three different nanoparticle concentrations (0.01, 0.05 & 0.1 wt. %) were dispersed into a eutectic salt mixture composed of 5.66% $NaNO_3$, 21.25% KNO_3, 24.75% $Ca(NO_3)_2$, 41% $CsNO_3$, & 7.34% $LiNO_3$ by weight. The results show that the graphene doping resulted in enhanced heat capacity ranging from 5 to 13%, whereas thermal conductivity increased marginally by ~3%, with respect to graphene concentration. Various theoretical models were tested to predict the thermal conductivity and heat capacity of the graphene-doped eutectic salt. The Maxwell and Hamilton-Crosser thermal conductivity models showed good agreement with experimental results, with a deviation of ± 3%, while Nan's thermal conductivity model over-predicted the thermal conductivity value. The conventional heat capacity equation fits well with the experimental data, with deviation < 14%.

1. Introduction

It is evident that fossil fuels are a non-renewable source of energy. As global energy demand and consumption continue to increase with modernization, finding alternate sources of energy has become inevitable. To balance the rapid increase in global energy consumption, we need to utilise renewable energy. There are many available renewable energy resources, such as solar, wind, geothermal and tidal energy, etc. Among these, solar energy is the most abundant, clean and easily available source of energy with an estimated 380 YW (1 Y = 10^{24}) of energy radiated by the sun [1]. To harness the solar energy many power plants have been constructed, for example, the Andasol and Arsenal power plants in Spain produce approximate energy of 158 GW h/yr, using parabolic trough collector technologies [2,3]. All the parabolic trough collectors use a 2-tank indirect heat exchange mechanism. In the first tank, a heat transfer fluid (HTF) such as eutectic salt is used. After melting, it flows from the collectors to a heat exchanger tank. In the second tank, water is used to produce steam, which is used to drive the turbine. Thus, by effectively utilising HTF, dependence on fossil fuels for electricity production can be reduced. HTF also functions as thermal energy storage (TES) material, and stores energy for a longer duration of time [4–6]. Eutectic salt is TES materials that include salts of hydrates, nitrates, and carbonates, and their eutectic mixtures. Eutectic salt possesses high thermal cycling stability; they are inexpensive and widely available. However, eutectic salts are slightly corrosive in nature and have low thermo-physical properties such as thermal conductivity [7–11].

Previous studies clearly demonstrate an enhancement in thermo-physical properties with the dispersion of nanomaterials in medium-high-temperature eutectic salt [12]. Andreu-Cabedo et al. [13]

Abbreviations: CNT, Carbon Nanotube; TES, Thermal Energy Storage; HTF, Heat Transfer Fluid; FPSC, Flat Plate Solar Collector; DSC, Differential Scanning Calorimetry; FESEM, Field Emission Scanning Electron Microscope; SEM, Scanning Electron Microscope; BSE, Back Scattered Electron; EDX, Energy Dispersive X-ray; TGA, Thermogravimetric Analysis

* Corresponding authors.
E-mail addresses: khalids@sunway.edu.my (M. Khalid), rashmi.walvekar@gmail.com (R. Walvekar).

https://doi.org/10.1016/j.materresbull.2019.110568
Received 12 April 2018; Received in revised form 13 July 2019; Accepted 26 July 2019
Available online 30 July 2019

Table 1
Mass composition of nitrate salts.

Salt	Amount (g)
$NaNO_3$	0.566
KNO_3	2.125
$LiNO_3$	0.734
$CsNO_3$	4.1
$CaNO_3$	2.475

dispersed silica (1 wt. %) nanoparticles in solar salt (60 wt. % $NaNO_3$ and 40 wt. % KNO_3) and reported a 25.03% enhancement in specific HC. Li et al. [14] obtained a 30% enhancement in specific heat capacity using HITEC salt (7 wt. % $NaNO_3$, 40 wt. % $NaNO_2$, and 53 wt. % KNO_3) by dispersing Sn/SiO_2 (5 wt. %) core-shell nanoparticles. Jo and Banerjee [15] claimed 40% (solid phase) and 57% (liquid phase) enhanced specific heat capacity by dispersing GE (0.1 wt. %) in binary carbonate salt (62:38 Li_2CO_3:K_2CO_3 by molar ratio). Thus, by dispersing nanomaterials in eutectic salt, thermal energy per unit volume can be increased significantly.

There are several theoretical models proposed for enhanced heat capacity. Critical analysis of heat capacity models has been performed by Khanafer et al. [16]. Various models have been presented for predicting the heat capacity of nanofluids [17]. The theoretical model described in Eq. (1) is based on the thermal equilibrium equation between the particle and base fluid [18].

$$C_{p,nf} = \frac{\rho_{np}\phi_{np}C_{p,np} + \rho_f\phi_f C_{p,f}}{\rho_{np}\phi_{np} + \rho_f\phi_f} \quad (1)$$

where ρ_{np} and ρ_f are the densities of nanoparticle and base fluid. ϕ_{np} and ϕ_f are the volume fractions of nanoparticle and base fluid, while $C_{p,nf}$, $C_{p,f}$ and $C_{p,np}$ are the heat capacity of nanofluid, base fluid and nanoparticle, respectively.

Eastman and coworker reported a dispersion of 5 vol. % CuO nanoparticles in water enhanced the thermal conductivity by 60% [19]. Another study reports that a 0.5% mass fraction of carbon nanotube (CNT) dispersed in glycol shows an 18% enhancement in thermal conductivity [20]. Many theories have been proposed to explain this anomalous enhancement in thermal conductivity, such as Brownian motion, nanoparticle clustering, uniform dispersion, liquid layers around nanoparticles [21,22]. Theoretical analysis for predicting enhanced thermal conductivity has been performed here by using the Maxwell, Hamilton-Crosser, and Nan models. Eq.s (2) and (3) represent the Maxwell and Hamilton-Crosser models.

$$k_{eff} = \frac{K_p + 2K_b + 2(K_p - K_b)\phi}{K_p + 2K_b - (K_p - K_b)\phi}K_b \quad (2)$$

where K_p and K_b are the thermal conductivity of the nanoparticle and base fluid respectively, ϕ is the nanoparticle volume fraction and K_{eff} is the effective thermal conductivity [23]. The Hamilton-Crosser model is a traditional model for predicting the thermal conductivity of heterogeneous solutions [24].

$$K_{eff} = \frac{K_p + (n_s - 1)K_f - (n_s - 1)\phi(K_f - K_p)}{K_p + (n_s - 1)K_f + \phi(K_f - K_p)}K_f \quad (3)$$

where K_p, K_f and K_{eff} are the thermal conductivity of the nanoparticles, thermal conductivity base fluid and the effective thermal conductivity of the nanofluid, respectively, n_s is the shape factor and ϕ is the nanoparticle volume fraction.

In analyzing the thermal behavior of the heterogeneous solution, Nan et al. [25] developed a new model for measuring the effective thermal conductivity of nanofluids, as shown in Eq.s (4) and (5) below.

$$K_{eff} = \frac{3 + \phi[2\beta_{11}(1 - L_{11}) + \beta_{33}(1 - L_{33})]}{3 - \phi(2\beta_{11}L_{11} + \beta_{33}L_{33})} \quad (4)$$

$$\beta_{ii} = \frac{K_p - K_{bf}}{K_{bf} + L_{ii}(K_p - K_{bf})} \quad (5)$$

where K_{eff} is the effective thermal conductivity. L_{ii} is the aspect ratio of graphene, and K_p and K_{bf} represent the thermal conductivity of the nanoparticle and base fluid, respectively.

This work focuses on two objectives: (i) the selection of low-melting-point eutectic salt, and (ii) enhancing the thermal properties of the selected eutectic salt. In this work, a eutectic mixture was selected on the basis of (i) its low melting point of 65 °C, (ii) it's high thermal stability > 500 °C, and (iii) its heat capacity > 1.18 J/g. °C. Although there are other eutectic mixtures, such as are given in Ahmed et al. [12], the advantages of using $CsNO_3$ are that: (i) it reduces melting point, viscosity, and maximizes the operating temperature of the eutectic mixture, and (ii) the heat capacity of $CsNO_3$ will increase with respect to temperature [26]. The main disadvantage of using $CsNO_3$ is that the overall cost of the eutectic mixture increases. The combination of selected nitrate salts ($NaNO_3$, KNO_3, $LiNO_3$, $CsNO_3$ and $CaNO_3$) were the focus of this study as it can be applied to both low and high temperature heat transfer applications [27]. Further, graphene sheets were selected as doping material because of their high thermal properties [28].

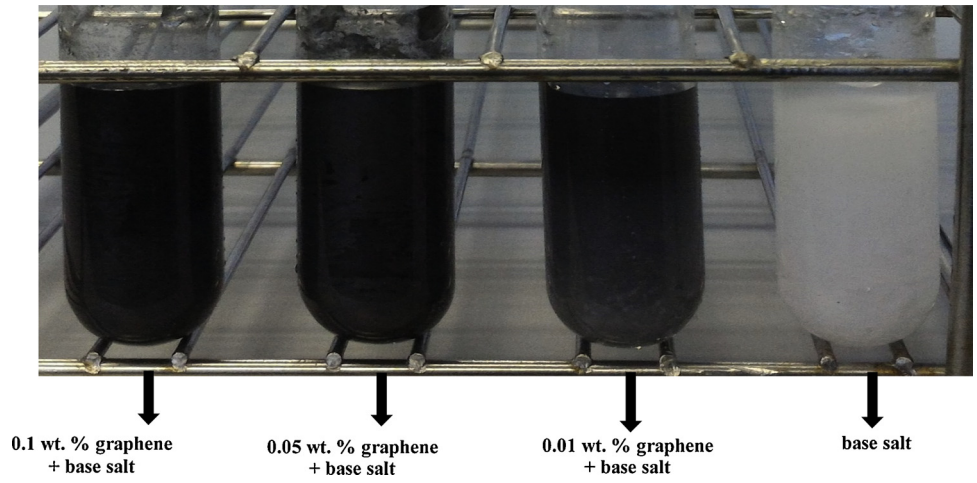

Fig. 1. Photograph of synthesized base salt along with dispersion of graphene concentrations.

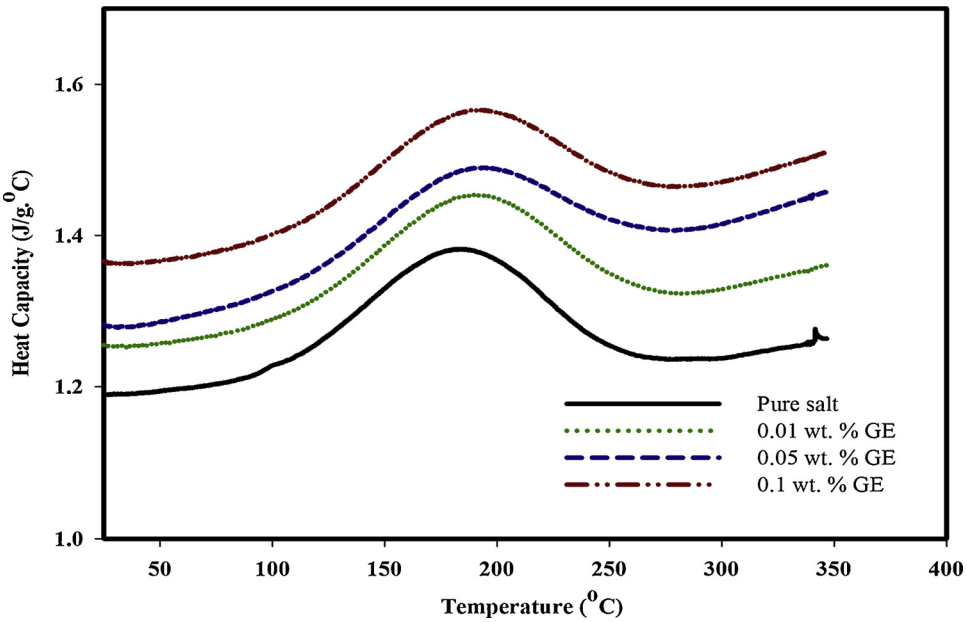

Fig. 2. HC of base salt mixed with different concentrations of grapheme.

Table 2
Enhanced heat capacity values with various concentrations of graphene in base eutectic salt.

Salt with various concentration of GE	Lowest HC	Highest HC value	Average HC	Enhanced HC
base salt	1.19 at 25 °C	1.38 at 185 °C	1.26	–
0.01 wt. %	1.25 at 25 °C	1.45 at 190 °C	1.34	5.065%
0.05 wt. %	1.28 at 25 °C	1.48 at 193 °C	1.39	7.525%
0.1 wt. %	1.36 at 25 °C	1.56 at 191 °C	1.46	13.169%

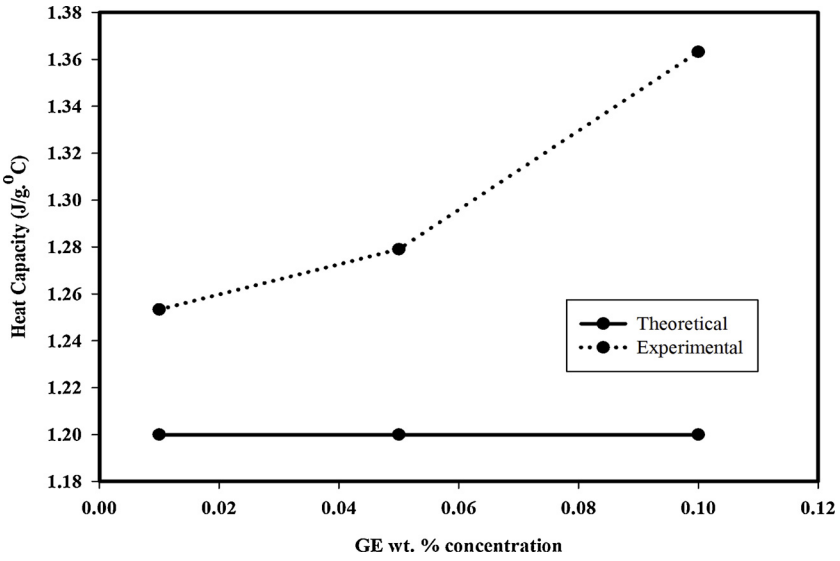

Fig. 3. Comparison of theoretical and experimental heat capacity with three concentrations of graphene (0.01, 0.05 and 0.1 wt. %).

2. Experimental procedure

Nitrate salts ($NaNO_3$, KNO_3, $LiNO_3$, $CsNO_3$ and $CaNO_3$) were procured from Sigma Aldrich, Germany. Multilayered graphene sheets of size 60 nm were purchased from Graphene Supermarket, USA. Each salt was mixed in the appropriate ratio to synthesize ~10 gm of eutectic salt, as shown in Table 1 [29]. The resultant eutectic salt was dissolved in 50 ml of deionized water with continuous stirring until all the salt was completely dissolved. Nano-suspensions were prepared by dispersing 0.01, 0.05 and 0.1 wt. % graphene into the eutectic salt.

The graphene nano-suspensions were ultra-sonicated using UP400S Hielscher ultrasound technology for 3 h, with a 5-min interval after every half hour of sonication. Amplitude and sweep cycle were maintained at 50% and 5 s, respectively. Afterward, the nano-suspension was heated on a hotplate at a constant temperature of 200 °C to vaporize the deionized water. The resultant sample was collected as shown in Fig. 1 and characterized for thermal properties as described in later sections.

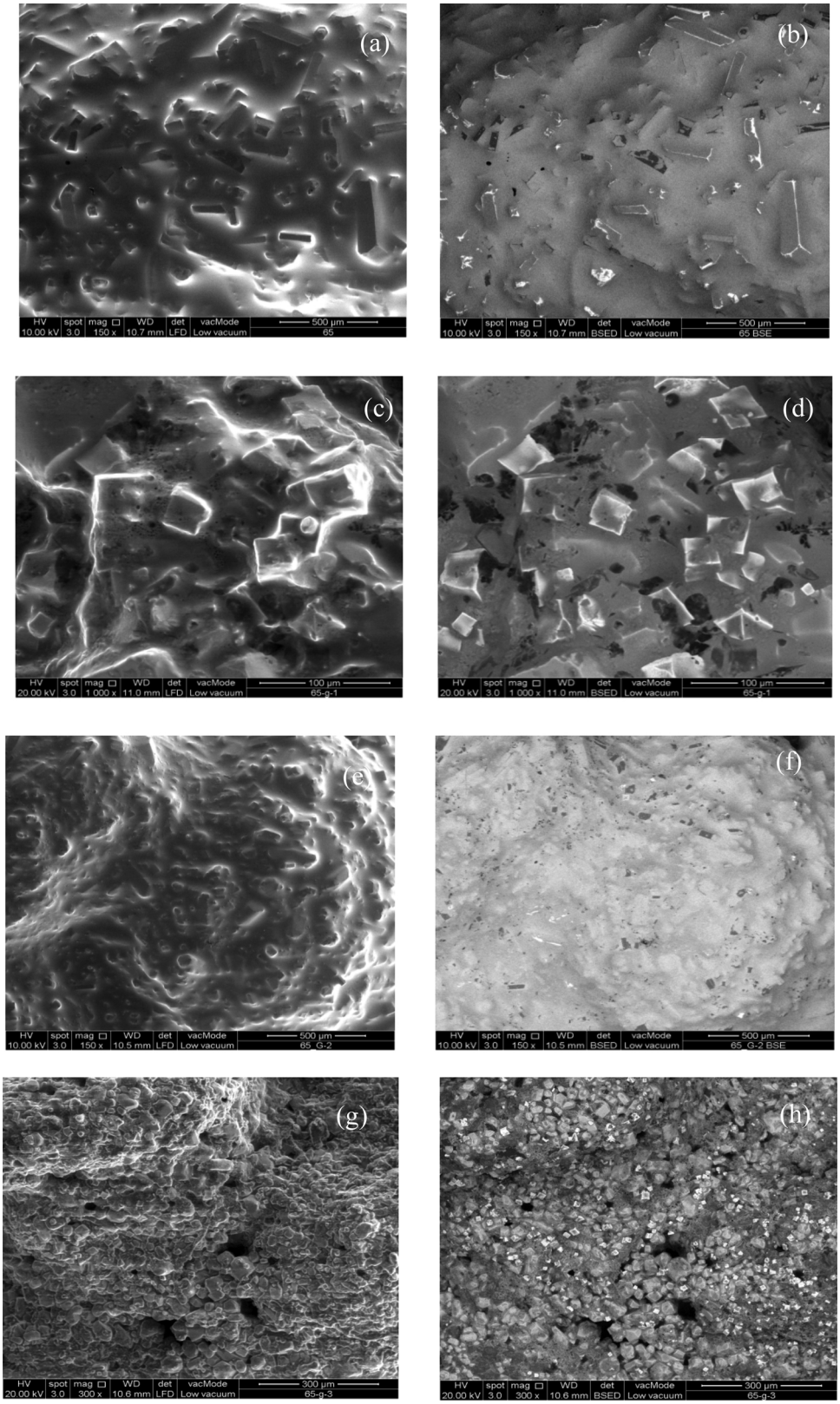

Fig. 4. (a), (c), (e), (g) are SEM and (b), (d), (f) and (h) are BSE images of base salt, 0.01 wt. %, 0.05 wt. % and 0.1 wt. % doped, graphene respectively.

3. Characterizations

Heat Capacity was measured using a differential scanning calorimeter (DSC) (TA instrument, Q2000 model) under a nitrogen atmosphere, with a flow rate of 20 ml/min. Tzero Hermetic aluminum pans and lids were used for DSC measurement. The samples were heated at 10 °C/min to 350 °C, to obtain HC values of the sample. The thermal properties of the eutectic salt dispersed with various concentrations of graphene were measured using thermogravimetric analysis (TGA) (Mettler Toledo, STARe model). All eutectic salts were heated under a

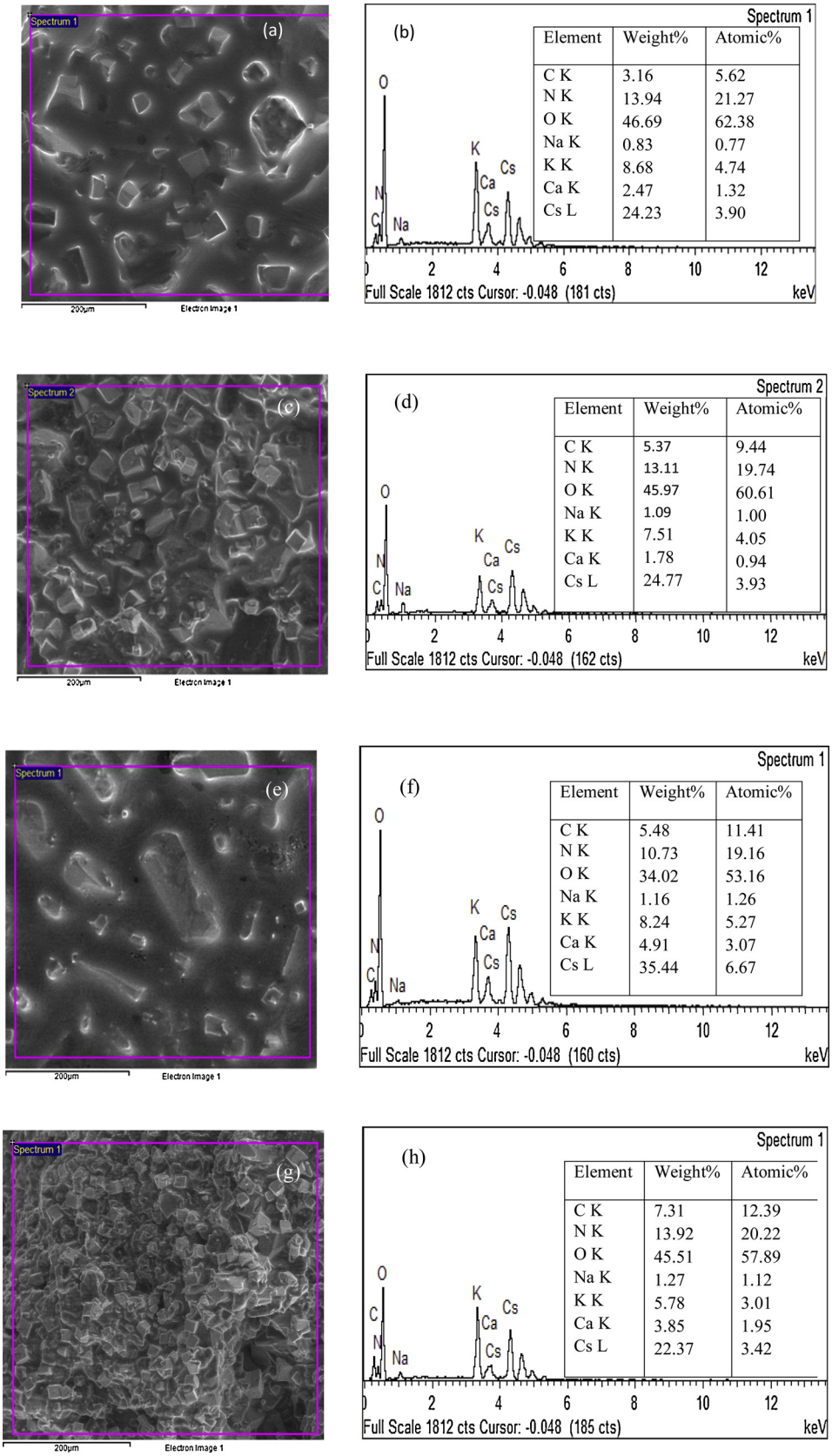

Fig. 5. (a), (c), (e) and (g) are SEM images, where EDX pattern had scanned. (b), (d), (f) and (h) are the EDX pattern of the base salt and with different concentrations of graphene.

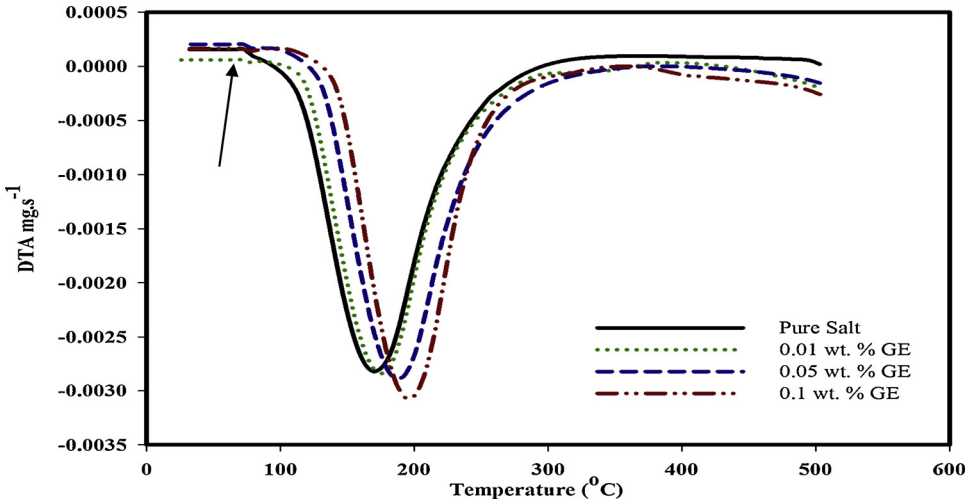

Fig. 6. Differential thermogravimetric analysis curve of base salt with different concentrations of graphene.

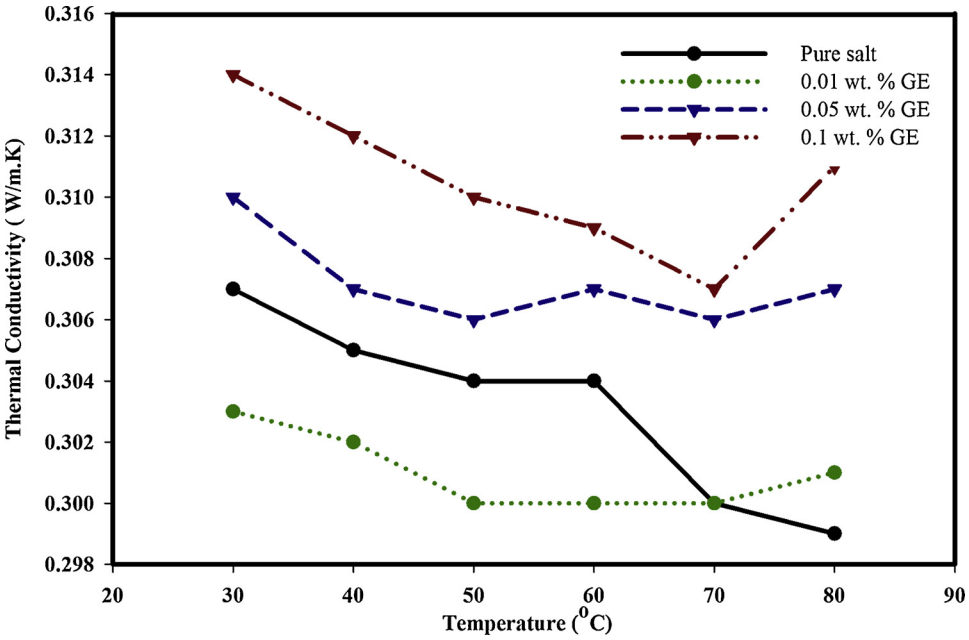

Fig. 7. Thermal conductivity of base eutectic salt with different concentrations of graphene (0.01, 0.05 and 0.1 wt. %).

nitrogen atmosphere from room temperature to 500 °C, with a ramp rate of 10 °C/min. FESEM (Quanta 400 F model) was used for morphological studies of base and graphene dispersed eutectic salt. Energy-dispersive X-ray (EDX) spectrometry was used for the elemental composition of the samples using Oxford Instruments (INCA 400 with X-max detector). Thermal conductivity of the samples was measured using a KD2 Pro thermal properties analyzer. The KD2 Pro equipment was programmed to get thermal conductivity readings every 15 min. However, limitations of the KD2 Pro thermal properties analyzer are that it operates within a temperature range of -50 to 150 °C. In this study, the sample temperature was not increased above 80 °C due to the large deviation in the thermal conductivity values (> 0.0099) due to convection. It is required to keep the sample stationary and stable during the measurement. Therefore, the temperature range for thermal conductivity studies was restricted between 30–80 °C. For every temperature, three readings were recorded, and the mean of these readings was noted.

4. Results and discussion

4.1. Differential scanning calorimeter

Fig. 2 shows the effect of graphene concentration on the heat capacity of base eutectic salt. It was observed that heat capacity was increased with increasing concentration of graphene. The average enhancement in heat capacity varied from 5 to 13%, with respect to graphene concentration. The heat capacity obtained for various samples is tabulated in Table 2, as shown below.

From Table 2, it is clear that heat capacity is a linear function of graphene concentration. The enhanced heat capacity of nano-suspensions is due to the following reasons: (i) reduced inter-crystal spacing due to the presence of graphene, (ii) a new mechanism of semi-solid behavior was expected to appear at the interaction between graphene and eutectic salt. This semi-solid behavior possesses high thermal properties than liquid [30].

4.1.1. Theoretical analysis of heat capacity

Fig. 3 gives a comparison of theoretical and experimental analyses

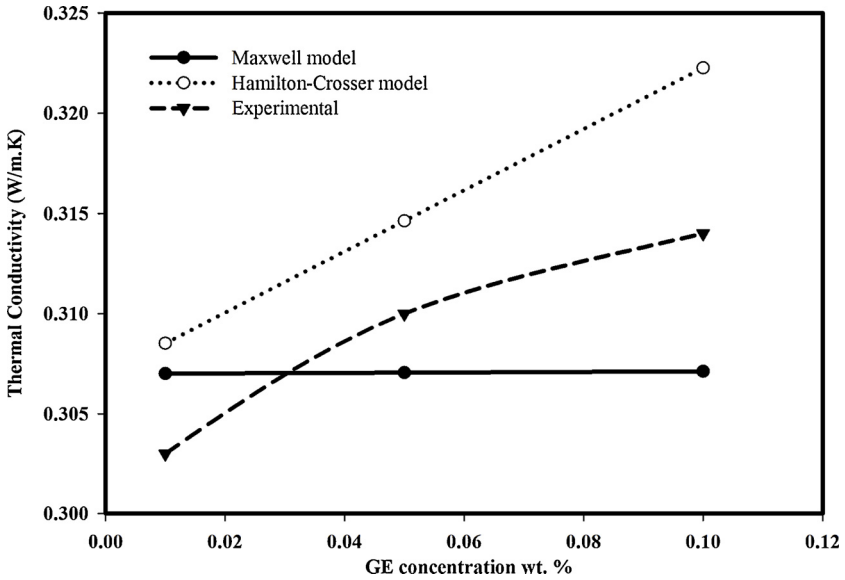

Fig. 8. Comparison of experimental thermal conductivity results with the Maxwell and Hamilton-Crosser models with respect to graphene concentration at room temperature.

Table 3
List of variables used in Maxwell and Hamilton-Crosser models.

Variable	Value
Kp	5200 W/m.K
Kf	0.307 W/m.K
ϕ (10^{-5})	1.34751, 6.73721 and 13.4735
n_s	375

of heat capacity. The density and heat capacity of the eutectic salt was measured to be 2.708 g/cm^3 and 1.19 J/g. °C and the density and heat capacity of graphene used were 2 g/cm^3 and 0.71 J/g. °C respectively. The density of the eutectic salt was measured using the conventional (mass/volume) method.

The experimental values are in good agreement with the theoretical values, having deviations of 4.44%, 6.58% and 13.60% for 0.01, 0.05 and 0.1 wt. % graphene, respectively. This deviation occurred because the above model does not take into consideration temperature, thickness, or size of the graphene. However, the authors suggest that improvement in Eq. (1) can be achieved by superposition of the individual heat capacity of the base fluids and nanomaterial.

4.2. Field emission scanning Electron microscope (FESEM)

Fig. 4 shows scanning electron microscope (SEM) and back-scattered electron (BSE) images of the base salt and the graphene-doped eutectic salt. Generally, BSE is used for identifying various elements in the samples through contrast differences. From Fig. 4, it can be observed that all the samples absorbed moisture while placed in the FESEM chamber. As all nitrate salts are hygroscopic in nature, and eutectic mixing of nitrate salts makes their hygroscopic nature more drastic, it was difficult to obtain clear SEM and BSE images of the samples.

4.2.1. Energy dispersive X-ray (EDX) analysis

From the BSE characterizations, the contrast difference between the

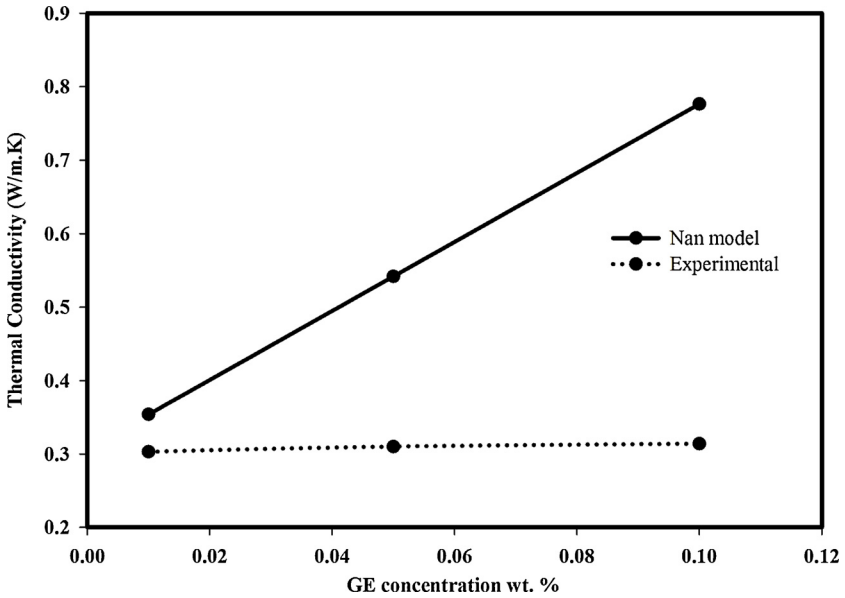

Fig. 9. Comparison of experimental results with Nan's model prediction for 0.01, 0.05 and 0.1 wt. % of graphene concentrations at room temperature.

various elements cannot be clearly seen, due to the hygroscopic nature of eutectic salt. Therefore, EDX was used for determining the elemental composition of the samples. The purple line in Fig. 5 is the area scanned for EDX analysis. From the peaks, it was found that all elements of eutectic salt are available, except Li. As EDX detects elements heavier than Be, it can also be observed through weight composition that the carbon (C) quantity was very low for the base salt. Gradually, the amount of carbon was increased with respect to the graphene concentration.

4.3. Differential thermogravimetric analysis

Differential thermogravimetric analysis (DTGA) of the base eutectic salt with different concentrations (0.01, 0.05 and 0.1 wt. %) of graphene is shown in Fig. 6. The first change in peak occurred due to glass transition (solid to liquid) of eutectic salt at 65 °C. The second weight loss peak around 80 °C was due to the evaporation of the moisture content. Based on DTGA results, all eutectic and graphene doped eutectic salt's endothermic reaction started in the range from 65 to 70 °C. After the endothermic reaction, the peak recovers, which means that there was no decomposition of any nitrate salt. Phase changes of eutectic salt and graphene doped eutectic salt are at 65 °C. This means that the various concentration of graphene in eutectic salt did not undergo phase transition process. It was eutectic salt that accounted for any changes in phase transition. From Fig. 6, it was also observed that all the synthesized eutectic salts were thermally stable up to 500 °C. Therefore, it could be inferred that the eutectic salts could be safely used within a range of 500 °C. Similar results were also reported by Wang et al. [31] for $LiNO_3$–$NaNO_3$–KNO_3 ternary system.

4.4. Thermal conductivity

The effect of the graphene addition upon thermal conductivity is depicted in Fig. 7. The thermal conductivity of the base salt decreased with increasing temperature. With the addition of 0.01 wt. % graphene in the eutectic salt, initially the thermal conductivity decreased until 50 °C, remained almost constant up to 70 °C, and started to increase from 70 °C. However, the enhanced thermal conductivity for 0.05 and 0.1 wt. % graphene compared to the base salt depicted a similar trend of the initial decrease in thermal conductivity with temperature until 70 °C and started to increase after 70 °C. There was an increase in thermal conductivity enhancement by 1.32 and 2.31% with doping graphene of 0.05 and 0.1 wt. %, respectively. The improvement in thermal conductivity was due to the high thermal conductivity and Brownian motion of the graphene [32]. Another reason for the improvement in thermal conductivity was due to the percolation network of graphene at higher concentration [33]. Several thermal conductivity models, like Maxwell's, Hamilton-Crosser's, and Nan's models, are also discussed in later sections.

4.4.1. Maxwell and Hamilton-Crosser models

Predicting the thermal conductivity values of eutectic salt doped with graphene are studied here using the Maxwell and Hamilton-Crosser models. Fig. 8 shows the comparison between the effective thermal conductivity of the Maxwell model, the Hamilton-Crosser model, and experimental results at room temperature. Table 3 shows a list of variables and their values used in the theoretical models. It was observed that both the Maxwell and Hamilton-Crosser models are very close to the experimental results. The deviation of error for both the Maxwell and Hamilton-Crosser models is between ± 3%. These two models take into consideration the individual thermal conductivity and volume fraction values, making them more robust with better accuracy. Khanafer and Vafai [34] observed that the Hamilton-Crosser model gives a good prediction of thermal conductivity with a volume fraction of nanomaterials ≤ 4%. Hence, predicting the thermal conductivity values of eutectic salt doped with graphene is in good agreement with experimental results. Authors point out that the accuracy of predicted thermal conductivity values increases if the measured thermal conductivity values taken in a liquid state.

4.4.2. Nan model of thermal conductivity

Nan et al. [25] have developed a thermal conductivity model for CNT-based fluids, as presented in Eq.s (4) and (5). In Nan's model, the aspect ratio of graphene was used. Fig. 9 shows a comparison of Nan's model with measured experimental results at room temperature. It was observed that Nan's model significantly over-predicted the experimental data. The error of deviation exponentially increased with respect to the addition of graphene concentration. This discrepancy was because of the graphene sheet thickness, as Nan's model does not take graphene thickness into consideration. Another reason for the enhanced thermal conductivity of Nan's model was that Eq. (4) is largely dependent on the change in volume fraction [35]. Furthermore, Nan's model also does not account the effect of temperature, Brownian motion and other underlying mechanisms which limits the Nan's model being applied under this case.

5. Conclusion

This study has focused on investigating the thermal properties of low-temperature eutectic salt doped with three different concentrations of graphene. Dispersing 0.01, 0.05 and 0.1 wt. % of graphene in the base eutectic salt led to enhanced heat capacity by 5.065, 7.525, and 13.169%, respectively. This enhancement in heat capacity with the addition of graphene was due to the reduced inter-layer spacing between eutectic salt molecules. The conventional theoretical model of heat capacity was in good agreement with the experimental results, as the error of deviation was < ± 14. Moreover, enhancement of 1.32 and 2.31% in TC was observed with the addition of 0.05 and 0.1 wt. % graphene, respectively. This enhanced thermal conductivity is due to the Brownian motion and percolation network of the graphene. Further, various theoretical thermal conductivity models were used to predict the experimental thermal conductivity values. The Maxwell and Hamilton-Crosser models were found to be in good agreement with experimental results. However, Nan's model did not fit the experimental results. Thus, enhancement in thermal properties of graphene doped eutectic salt makes it a feasible option to use as TES material than base eutectic salt.

Acknowledgement

The authors would like to acknowledge Taylor's University Flagship Research grant (TUFR/2017/001/01) for this project.

References

[1] S.A. Kalogirou, Solar thermal collectors and applications, Prog. Energy Combust. Sci. 30 (3) (2004) 231–295.
[2] Andasol-1, < http://www.nrel.gov/csp/solarpaces/project_detail.cfm/projectID = 3 > . 2017 [accessed 09.10.17].
[3] Arenales, < http://www.nrel.gov/csp/solarpaces/project_detail.cfm/projectID = 241 > . 2017 [accessed 09.10.17].
[4] X. Min, et al., Enhanced thermal properties of novel shape-stabilized PEG composite phase change materials with radial mesoporous silica sphere for thermal energy storage, Sci. Rep. 5 (2015) 12964.
[5] Y. Zhao, et al., Honeycomb-like structured biological porous carbon encapsulating PEG: a shape-stable phase change material with enhanced thermal conductivity for thermal energy storage, Energy Build. 158 (2018) 1049–1062.
[6] X. Zhang, et al., Preparation and characterization of the properties of polyethylene glycol @ Si3N4 nanowires as phase-change materials, Chem. Eng. J. 301 (2016) 229–237.
[7] A.J. Chamkha, et al., Phase-change heat transfer of single/hybrid nanoparticles-enhanced phase-change materials over a heated horizontal cylinder confined in a square cavity, Adv. Powder Technol. 28 (2) (2017) 385–397.
[8] A. Doostanidezfuli, M. Ghalambaz, A. Chamkha, MHD natural convection phase-change heat transfer in a cavity: analysis of the magnetic field effect, J. Braz. Soc. Mech. Sci. Eng. 39 (2017).
[9] M. Ghalambaz, et al., Melting of nanoparticles-enhanced phase-change materials in

an enclosure: effect of hybrid nanoparticles, Int. J. Mech. Sci. 134 (2017) 85–97.
[10] M. Ghalambaz, et al., Phase-change heat transfer in a cavity heated from below: the effect of utilizing single or hybrid nanoparticles as additives, J. Taiwan Inst. Chem. Eng. 72 (2017) 104–115.
[11] H. Zargartalebi, et al., Natural convection of a nanofluid in an enclosure with an inclined local thermal non-equilibrium porous fin considering Buongiorno's model, Numer. Heat Transf. Part A Appl. 70 (4) (2016) 432–445.
[12] S.F. Ahmed, et al., Recent progress in solar thermal energy storage using nanomaterials, Renewable Sustainable Energy Rev. 67 (2017) 450–460.
[13] P. Andreu-Cabedo, et al., Increment of specific heat capacity of solar salt with SiO (2) nanoparticles, Nanoscale Res. Lett. 9 (1) (2014) p. 582-582.
[14] C.-C. Lai, et al., A solar-thermal energy harvesting scheme: enhanced heat capacity of molten HITEC salt mixed with Sn/SiOx core-shell nanoparticles, Nanoscale 6 (9) (2014) 4555–4559.
[15] B. Jo, D. Banerjee, Enhanced specific heat capacity of molten salt-based nanomaterials: effects of nanoparticle dispersion and solvent material, Acta Mater. 75 (0) (2014) 80–91.
[16] K. Khanafer, et al., A critical investigation of the anomalous behavior of molten salt-based nanofluids, Int. Commun. Heat Mass Transf. 69 (2015) 51–58.
[17] S.-Q. Zhou, R. Ni, Measurement of the specific heat capacity of water-based Al2O3 nanofluid, Appl. Phys. Lett. 92 (9) (2008) p. 093123.
[18] L.-P. Zhou, et al., On the specific heat capacity of CuO nanofluid, Adv. Mech. Eng. 2 (2010).
[19] J.A. Eastman, et al., Enhanced thermal conductivity through the development of nanofluids, MRS Online Proceedings Library 457 (1996) p. null-null.
[20] Z. Meng, et al., Carbon nanotube glycol nanofluids: photo-thermal properties, thermal conductivities and rheological behavior, Particuology 10 (5) (2012) 614–618.
[21] H.Ş. Aybar, et al., A review of thermal conductivity models for nanofluids, Heat Transf. Eng. 36 (13) (2015) 1085–1110.
[22] P. Keblinski, et al., Mechanisms of heat flow in suspensions of nano-sized particles (nanofluids), Int. J. Heat Mass Transf. 45 (4) (2002) 855–863.
[23] J.C. Maxwell, A Treatise on Electricity and Magnetism, Clarendon Press, 1873.
[24] R.L. Hamilton, O.K. Crosser, Thermal conductivity of heterogeneous two-component systems, Ind. Eng. Chem. Fundam. 1 (3) (1962) 187–191.
[25] C.W. Nan, Z. Shi, Y. Lin, A simple model for thermal conductivity of carbon nanotube-based composites, Chem. Phys. Lett. 375 (5–6) (2003) 666–669.
[26] H.E. Flotow, P.A.G. O'Hare, J. Boerio-Goates, Heat capacity from 5 to 350 K and thermodynamic properties of cesium nitrate to 725 K, J. Chem. Thermodyn. 13 (5) (1981) 477–483.
[27] S.F. Ahmed, et al., Investigation of rheological and corrosion properties of graphene-based eutectic salt, J. Mater. Sci. 53 (1) (2018) 692–707.
[28] L.A. Jauregui, et al., Thermal transport in graphene nanostructures: experiments and simulations, ECS Trans. 28 (5) (2010) 73–83.
[29] Raade, J., B. ELKIN, and L. Finkelstein, Thermal energy storage with molten salt. Google Patents, 2013.
[30] D. Shin, D. Banerjee, Enhancement of specific heat capacity of high-temperature silica-nanofluids synthesized in alkali chloride salt eutectics for solar thermal-energy storage applications, Int. J. Heat Mass Transf. 54 (5–6) (2011) 1064–1070.
[31] T. Wang, D. Mantha, R.G. Reddy, Thermal stability of the eutectic composition in LiNO3–NaNO3–KNO3 ternary system used for thermal energy storage, Sol. Energy Mater. Sol. Cells 100 (0) (2012) 162–168.
[32] S.P. Jang, S.U.S. Choi, Role of Brownian motion in the enhanced thermal conductivity of nanofluids, Appl. Phys. Lett. 84 (21) (2004) 4316–4318.
[33] M. Shtein, et al., Thermally conductive graphene-polymer composites: size, percolation, and synergy effects, Chem. Mater. 27 (6) (2015) 2100–2106.
[34] K. Khanafer, K. Vafai, A critical synthesis of thermophysical characteristics of nanofluids, Int. J. Heat Mass Transf. 54 (19) (2011) 4410–4428.
[35] M. Mehrali, et al., Investigation of thermal conductivity and rheological properties of nanofluids containing graphene nanoplatelets, Nanoscale Res. Lett. 9 (1) (2014) 1–12.